Effects of Ge substitution in GeTe by Ag or Sb on the Seebeck coefficient and carrier concentration derived from ^{125}Te NMR

E. M. Levin[*]

U.S. Department of Energy Ames Laboratory, Division of Materials Sciences and Engineering, Ames, Iowa 50011, USA
and Department of Physics and Astronomy, Iowa State University, Ames, Iowa 50011, USA

GeTe, a self-doping p-type semiconductor where the high free hole concentration is determined by Ge vacancies is a well-known base for high-efficiency $Ag_xSb_xGe_{50-2x}Te_{50}$ (a tellurium-antimony-germanium-silver series) thermoelectric materials. Here it is shown that the replacement of Ge by Ag in GeTe (a $Ag_xGe_{50-x}Te_{50}$ system) significantly decreases the Seebeck coefficient, whereas the replacement by Sb ($Sb_xGe_{50-x}Te_{50}$) increases it. These effects can be attributed to a change in carrier concentration and consistent with ^{125}Te NMR spin-lattice relaxation measurements and NMR signal position, which is mostly dependent on the Knight shift. Opposite changes in carrier concentration in $Ag_xGe_{50-x}Te_{50}$ and $Sb_xGe_{50-x}Te_{50}$ can be explained by different valence electron configurations of Ag and Sb compared to that of Ge, which results in a different local electron imbalance and/or in a change in Ge vacancy formation energy and affects the total carrier concentration. Comparison of our data for GeTe, $Ag_2Ge_{48}Te_{50}$, and $Sb_2Ge_{48}Te_{50}$ with those for $Ag_2Sb_2Ge_{46}Te_{50}$ shows that the effects from Ag and Sb compensate for each other and supports the formation of [Ag + Sb] atomic pairs suggested earlier based on theoretical calculations.

Thermoelectric materials convert thermal energy to electricity via the Seebeck effect, a very interesting fundamental phenomenon observed in electrically conductive solids [1]. One well-known group of high-efficiency thermoelectric materials is based on GeTe where Ge is replaced by Ag and Sb forming $Ag_xSb_xGe_{50-2x}Te_{50}$ [tellurium-antimony-germanium-silver (TAGS)] materials [2]. These materials show p-type (hole) conductivity and continue to attract great attention [3–5], whereas the origin of their high efficiency has never been explained. GeTe is a p-type narrow-band semiconductor [6] with a high hole concentration $8 \times 10^{20} cm^{-3}$, generated by $\sim 4 \times 10^{20} cm^{-3}$ Ge vacancies (each Ge vacancy generates two holes) [7,8] and exhibits a gradual transformation of a low-temperature rhombohedral to a high-temperature cubic structure [8,9], which makes this compound a very complex solid-state system.

The Seebeck coefficient (or thermopower) S and electrical resistivity ρ are used to estimate the power factor $PF = S^2/\rho$, which is a part of the thermoelectric figure of merit. Both the Seebeck coefficient and the electrical resistivity are very sensitive to mobile charge-carrier concentration, which can be controlled via chemical substitution. The goal of this paper is to elucidate the effects of local electron imbalance on the Seebeck coefficient, electrical resistivity, power factor, and carrier concentration obtained from ^{125}Te nuclear magnetic resonance (NMR) in GeTe-based materials where Ge is partially replaced by Ag ($Ag_xGe_{50-x}Te_{50}$ alloys) or Sb ($Sb_xGe_{50-x}Te_{50}$) and to compare the results to those in $Ag_2Sb_2Ge_{46}Te_{50}$.

Individual ingots of all alloys with diameters of 10 mm and lengths of ~ 40 mm were synthesized by the direct melting of the components in fused quartz ampoules at 1323 K. X-ray diffraction (XRD) patterns were obtained using a Rigaku Ultima U4 diffractometer at 300 K. Homogeneity and composition of all alloys were checked by scanning electron microscopy (SEM) and energy dispersive spectroscopy (EDS). ^{125}Te NMR experiments were performed at 126 MHz using a Bruker 400WB plus spectrometer with TOPSPIN software in a magnetic field of 9.4 T without sample spinning (static regime). ^{125}Te NMR chemical shifts were referenced to Te(OH)$_6$ in solution, and chemical shifts relative to (CH$_3$)$_2$Te in benzene were larger by $+712$ ppm (parts per 10^6) [10]. ^{125}Te NMR spin-lattice relaxation measurements were used to obtain the spin-lattice relaxation time T_1 and free (mobile) charge-carrier concentration p using GeTe as a reference material [8,10]. Measurements of the Seebeck coefficient and electrical resistivity were conducted simultaneously on the same sample using a LSR-3 measuring system (Linseis, Inc.) in a helium environment. Uncertainties in T_1 and p measurements are 2% and 10%, respectively, whereas uncertainties in the Seebeck coefficient and electrical resistivity measurements are less than 5% and 3%, respectively. More details about sample preparation, XRD, ^{125}Te NMR, Seebeck coefficient, electrical resistivity, SEM, and EDS measurements can be found in Refs. [5,8,10].

XRD shows that the replacement of Ge by Ag or Sb in GeTe can be represented by idealized solid solution compositions of $Ag_xGe_{50-x}Te_{50}$ or $Sb_xGe_{50-x}Te_{50}$ with an average composition close to the nominal. XRD shows the presence of a small amount of Ge inclusions in Sb-containing samples but not in Ag-containing samples. SEM and EDS confirm the presence of small amounts of Ge (<2 at. %) inclusions in Sb-containing samples, similar to that observed in GeTe [8], and to a smaller extent in Ag-containing samples. In addition, EDS shows that the concentrations of Ag and particularly Sb in these materials slightly vary along the sample reflecting their inhomogeneity.

Figure 1 presents temperature dependencies of the Seebeck coefficient of $Ag_xGe_{50-x}Te_{50}$ and $Sb_xGe_{50-x}Te_{50}$ alloys with $x = 2$ and 4. No hysteresis in the Seebeck coefficient and electrical resistivity (both have been measured but are not shown here) during temperature cycling was observed.
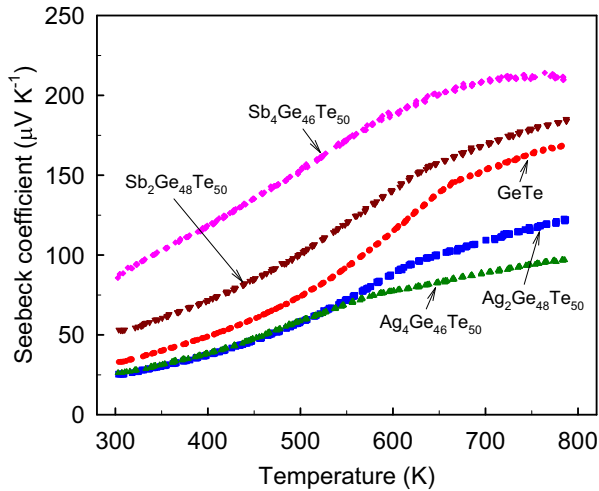
———————
*levin@iastate.edu

FIG. 1. Temperature dependences of the absolute Seebeck coefficient of $Ag_xGe_{50-x}Te_{50}$ and $Sb_xGe_{50-x}Te_{50}$ alloys. Data for GeTe are shown for comparison.

Figure 2 demonstrates trends in S and ρ vs Ag or Sb content in $Ag_xGe_{50-x}Te_{50}$ and $Sb_xGe_{50-x}Te_{50}$ alloys at 300 and 750 K (see also Table I). It is interesting that at 750 K, the Seebeck coefficient of $Ag_2Sb_2Ge_{46}Te_{50}$ containing 4 at. % of [Ag + Sb] shows a value close to that of GeTe, but higher than that of $Ag_4Ge_{46}Te_{50}$, and lower than that of $Sb_4Ge_{46}Te_{50}$ (Table I). Within the Mott-Boltzmann formalism for systems with energy-independent charge-carrier scattering, the Seebeck coefficient depends on the carrier concentration n of electrons or holes as $S \sim 1/n^{2/3}$ (e.g., see Ref. [1]). The carrier concentration in semiconductors typically is deduced from Hall effect measurements. However, the Hall effect in multicomponent materials can be misleading due to the possible presence of separate phases particularly with different types of conductivity. For example, the Hall effect in p-type $AgSbTe_2$ shows n type, which was attributed to the small amount of n-type Ag_2Te, whereas the Seebeck effect shows p type, reflecting the major phase [11]. Potentially more reliable values of the carrier concentration and its distribution can be obtained from ^{125}Te NMR spin-lattice relaxation measurements [10]. The Hall effect shows an integral signal from all phases or local areas with nonuniform carrier concentration in a material, whereas ^{125}Te NMR shows differential signals from each phase or local areas. This enables a better understanding of the Seebeck effect, which, similar to the Hall effect, shows an integral signal from all phases or local areas. Note that in complex tellurides, local variation in chemical composition (although this cannot be detected by XRD) results in a variation of the Seebeck coefficient, which can be attributed to the variation in carrier concentration and similar to the Hall effect can be misleading (see discussion below).

Figure 3 shows ^{125}Te NMR spectra for GeTe (which confirm the position and shape of the NMR signal for this compound reported in Refs. [8,10]) and several $Ag_xGe_{50-x}Te_{50}$ and $Sb_xGe_{50-x}Te_{50}$ samples. Replacement of Ge by Ag shifts the signal from +160 ppm for GeTe to more positive values whereas the replacement of Ge by Sb shifts the signal to
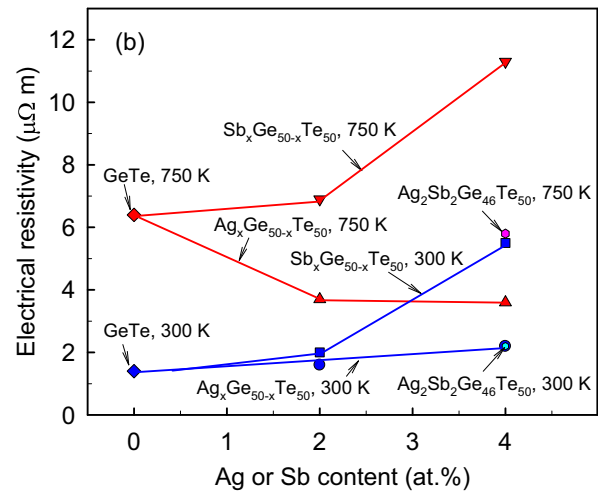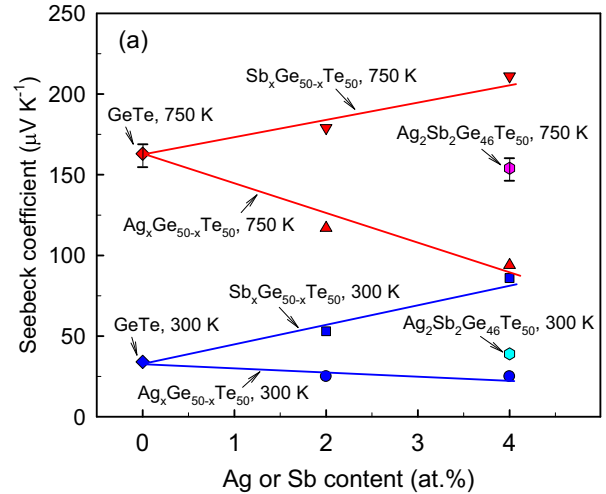

FIG. 2. Dependencies of the (a) Seebeck coefficient and (b) electrical resistivity of $Ag_xGe_{50-x}Te_{50}$ and $Sb_xGe_{50-x}Te_{50}$ at 300 and 750 K vs Ag or Sb content. Data for $Ag_2Sb_2Ge_{46}Te_{50}$ are shown for comparison.

more negative values (Table I). The ^{125}Te NMR signal for $Ag_2Sb_2Ge_{46}Te_{50}$, similar to that reported in Ref. [12], is observed at +320 ppm, which is an intermediate value between those observed if only Ag or Sb atoms are present in the crystal lattice. Note that if Ag and Sb in the $Ag_2Sb_2Ge_{46}Te_{50}$ lattice are located far from each other, the FWHM of the ^{125}Te NMR signal, estimated for $Ag_2Sb_{48}Te_{50}$ and $Sb_2Ge_{48}Te_{50}$ (see Fig. 3), is expected to be large $\sim 1200\,ppm$. In reality, the ^{125}Te NMR signal for $Ag_2Sb_2Ge_{46}Te_{50}$ shows a much smaller FWHM = 510 ppm (Table I).

Comparison of our ^{125}Te NMR and the Seebeck coefficient data for GeTe, $Ag_2Ge_{48}Te_{50}$, and $Sb_2Ge_{48}Te_{50}$ with those for $Ag_2Sb_2Ge_{46}Te_{50}$ shows that effects from Ag and Sb nearly compensate for each other. This can be explained: (i) by the opposite effect (compensation) from Ag and Sb or (ii) by the formation of [Ag + Sb] atomic pairs. Note that the Seebeck coefficient of $Ag_xSb_xGe_{50-2x}Te_{50}$ with $x \approx 6.5$ is very large compared to that of GeTe, +83 and +193 $\mu V\,K^{-1}$ at 300 and 750 K, respectively (similar large values were reported in Refs. [3,4]), which means that there is no compensation

TABLE I. Composition, Seebeck coefficient S, electrical resistivity ρ, ^{125}Te NMR peak position (i.e., the total shift δ_{total}), full width at half maximum (FWHM), spin-lattice relaxation time T_1, and the carrier concentration p, obtained from T_1 using Maxwell-Boltzmann statistics.

Composition	S (μV K^{-1})		ρ ($\mu\Omega$ m)		δ_{total} (ppm)	FWHM (ppm)	Spin-lattice relaxation time[a] and fraction	p (cm^{-3})
	300 K	750 K	300 K	750 K	300 K	300 K	300 K	300 K
GeTe	+34	+163	1.4	6.4	+160	460	$T_1 = 5.3$ ms	8×10^{20}
Ag$_2$Ge$_{48}$Te$_{50}$	+26	+116	1.6	3.7	+620	480	$T_1 = 2.0$ ms	20×10^{20}
Ag$_4$Ge$_{46}$Te$_{50}$	+25	+94	2.2	3.6	+730	530	$T_1 = 1.6$ ms	25×10^{20}
Sb$_2$Ge$_{48}$Te$_{50}$	+53	+180	2.0	6.9	−30	550	$T_{1,A} = 3.2$ ms, $f_A = 0.68$	14×10^{20}
							$T_{1,B} = 19.0$ ms, $f_B = 0.32$	2×10^{20}
Sb$_4$Ge$_{46}$Te$_{50}$	+86	+211	4.2	10.8	−460	550	$T_{1,A} = 3.0$ ms, $f_A = 0.39$	14×10^{20}
							$T_{1,B} = 30.0$ ms, $f_B = 0.61$	1.4×10^{20}
Ag$_2$Sb$_2$Ge$_{46}$Te$_{50}$	+39	+154	2.2	5.5	+320	510	$T_1 = 3.6$ ms	12×10^{20}

[a]Can be fit by one T_1 or two components $T_{1,A}$ and $T_{1,B}$ with fractions f_A and f_B.

from Ag and Sb here and is in favor of the existence of [Ag + Sb] pairs. Such pairs and a gradual transformation of the crystal structure from rhombohedral to cubic [8,9] can be responsible for the high efficiency of TAGS materials. Possible formation of [Ag + Sb] pairs in GeTe was theoretically studied by Hoang *et al.* [13] as well as in PbTe by Hazama *et al.* [14]; our ^{125}Te NMR data support these theoretical calculations.
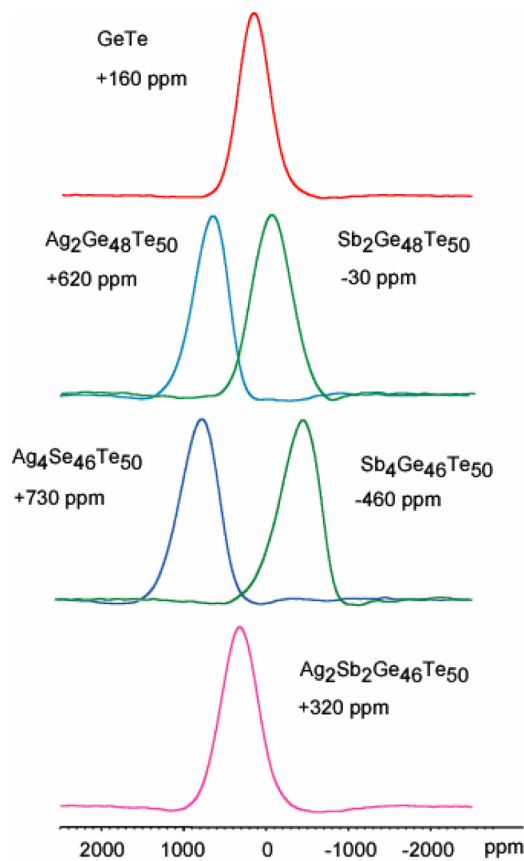

FIG. 3. ^{125}Te NMR spectra (static regime) of p-type GeTe, Ag$_x$Ge$_{50-x}$Te$_{50}$, Sb$_x$Ge$_{50-x}$Te$_{50}$, and Ag$_2$Sb$_2$Ge$_{46}$Te$_{50}$ at 300 K obtained for 50-ms saturated recovery time.

Spin-lattice relaxation in Ag$_2$Ge$_{48}$Te$_{50}$ can be fit mostly by one component $T_1 = 2.0$ ms as well as in Ag$_4$Ge$_{46}$Te$_{50}$ by $T_1 = 1.6$ ms, meaning that these alloys are mostly electronically and chemically homogeneous. In contrast, spin-lattice relaxation in Sb$_2$Ge$_{48}$Te$_{50}$ can be fit by two components $T_{1,A} = 3.2$ ms and $T_{1,B} = 19.0$ ms with fractions $f_A = 0.68$ and $f_B = 0.32$ (see details for fitting in Refs. [10,12]). A similar situation is observed for Sb$_4$Ge$_{46}$Te$_{50}$ with $T_{1,A} = 3.0$ and $T_{1,B} = 30$ ms with fractions $f_A = 0.39$ and $f_B = 0.61$, meaning that these alloys are electronically inhomogeneous.

Nonuniform carrier concentration in tellurides was suggested for PbTe-based materials based on microscale Seebeck scanning [15,16]. XRD, SEM, and EDS show chemically homogeneous materials, but Seebeck scanning demonstrates a significant change in its magnitude and even the presence of areas with n- or p-type conductivity [15]. This was explained by a possible change in carrier concentration due to slight local composition deviation [15,16], which for PbTe-based materials was also observed by ^{125}Te NMR [10,17]. Similar inhomogeneity for GeTe-based materials shown here demonstrates that the change in carrier concentration due to variation of local composition is typical for multicomponent tellurides.

The Seebeck coefficient of Sb$_2$Ge$_{48}$Te$_{50}$ is $+53 \, \mu$V K^{-1}, which is larger than that of GeTe, $+34 \, \mu$V K^{-1} (Table I). This difference shows that despite the fraction with lower carrier concentration in Sb$_2$Ge$_{48}$Te$_{50}$ is small $f_B = 0.32$, a possible contribution to the Seebeck coefficient from this fraction cannot be ignored and should be used to explain an increase in the Seebeck coefficient. It can be explained that the existence of areas with lower carrier concentration (and a larger Seebeck coefficient), which form series connections with areas of higher carrier concentration (and a lower Seebeck coefficient) along the temperature gradient, will result in a larger bulk (integral) Seebeck coefficient. Certainly, the bulk value depends on the spatial distribution of these areas. In Sb$_4$Ge$_{46}$Te$_{50}$, the fraction with the lower concentration is larger $f_B = 0.61$, and the bulk Seebeck coefficient is larger $+86 \, \mu$V K^{-1} (Table I), i.e., the contribution from the fraction with lower carrier concentration increases.
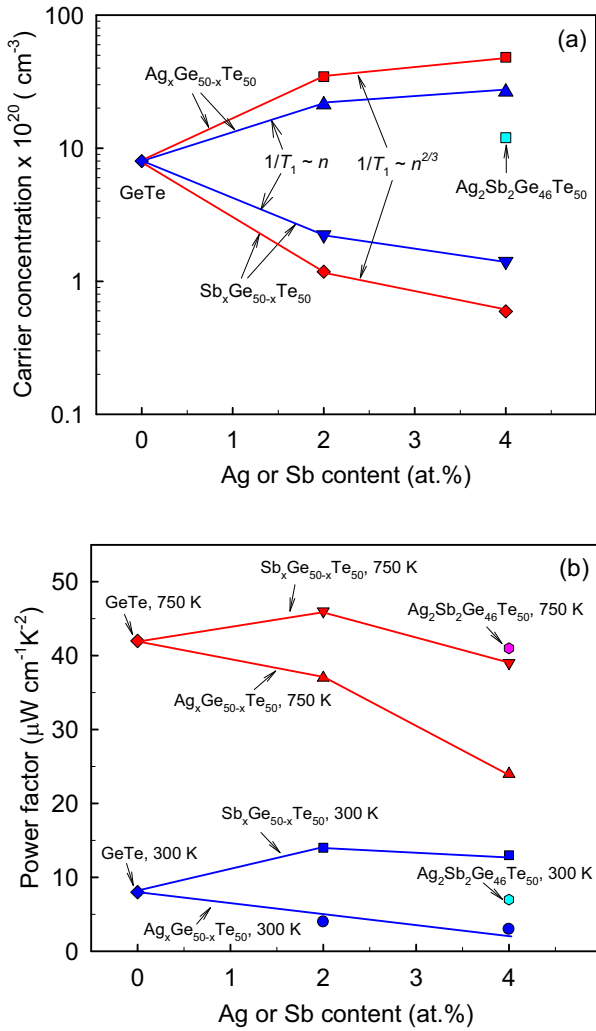
FIG. 4. (a) The carrier concentration obtained from ^{125}Te NMR spin-lattice relaxation measurements at 300 K using $1/T_1 \sim n$ (with Maxwell-Boltzmann statistics) and $1/T_1 \sim n^{2/3}$ (with Fermi-Dirac statistics) relations and (b) power factor of $Ag_xGe_{50-x}Te_{50}$ and $Sb_xGe_{50-x}Te_{50}$ vs Ag or Sb content at 300 and 750 K.

With Maxwell-Boltzmann statistics (used for semiconductors), the carrier concentration and spin-lattice relaxation time are related as $1/T_1 \sim n$, whereas with Fermi-Dirac statistics (used for metals) are related as $1/T_1 \sim n^{2/3}$ [18,19]. At the given temperature $n = n_r(T_{1,r}/T_1)$ (Maxwell-Boltzmann statistics) and using GeTe as a reference material with $T_{1,r} = 5.3 \pm 0.2$ ms from ^{125}Te NMR [8,10] and $p = 8 \times 10^{20}$ cm^{-3} from the Hall effect [7,8,20], we can calculate the corresponding hole concentration via the equation $p = 4.24 \times 10^{21}/T_1$ (T_1 in milliseconds, p in cm^{-3}) [10] in $Ag_2Ge_{48}Te_{50}$ and $Ag_4Ge_{46}Te_{50}$ [Fig. 4(a) and Table I]. The hole carrier concentrations estimated for $Sb_2Ge_{48}Te_{50}$ and $Sb_4Ge_{46}Te_{50}$ for a short and long T_1 are in general lower than that in Ag-containing samples [Fig. 4(a) and Table I]. The carrier concentrations in $Ag_xGe_{50-x}Te_{50}$ and $Sb_xGe_{50-x}Te_{50}$ calculated from T_1 using Fermi-Dirac statistics is different [see comparison in Fig. 4(a)], but the trends observed for these materials are the same: Ag increases the carrier concentration, whereas Sb decreases it. Hall effect measurements at 300 K

confirm this trend, showing that the carrier concentration in $Ag_xGe_{50-x}Te_{50}$ is higher, 17×10^{20} cm^{-3} ($x = 2$) and 30×10^{20} cm^{-3} ($x = 4$), compared to that in GeTe, and lower in $Sb_xGe_{50-x}Te_{50}$, 4×10^{20} cm^{-3} ($x = 2$) and 2.3×10^{20} cm^{-3} ($x = 4$), which are between those obtained from ^{125}Te NMR long and short T_1 (Table I). This shows that the high Hall voltage from the low-carrier concentration dominates the low Hall voltage from the high-carrier concentration, but the total Hall voltage is reduced.

It is possible to estimate changes in carrier concentration if Ge in GeTe is replaced by Ag or Sb. There are 1.85×10^{22} cm^{-3} Ge atoms in ideal GeTe. If one Ag atom replaces one Ge out of 50 in $Ge_{50}Te_{50}$ and results in one hole, the additional carrier concentration should be 3.7×10^{20} cm^{-3}; two Ag atoms result in 7.4×10^{20} cm^{-3}. The total concentration (background in GeTe is 8×10^{20} cm^{-3} plus the contribution due to two Ag) will be 15.4×10^{20} cm^{-3}. This value is close to that obtained from the Hall effect and ^{125}Te NMR spin-lattice relaxation measurements. Similarly, if one Sb atom replaces Ge and reduces the carrier concentration by one hole, the reduction due to two Sb atoms should be 7.4×10^{20} cm^{-3}, and the total carrier concentration should be reduced to 0.6×10^{20} cm^{-3}. This value is smaller compared to that obtained from NMR and Hall effect measurements and shows that Sb may have lower doping efficiency compared to Ag. The differences observed also can be attributed to the change in concentration of Ge vacancies: Ag can reduce the energy of the formation of a Ge vacancy, whereas Sb can increase it. Let us suggest that Ag and Sb affect only the concentration of Ge vacancies; note that there are $\sim 4 \times 10^{20}$ cm^{-3} (or $\sim 2\%$) naturally occurring Ge vacancies in GeTe. If Ag results in more Ge vacancies, $\sim 10 \times 10^{20}$ cm^{-3} (or $\sim 5\%$) Ge vacancies are needed to explain an increase in the carrier concentration in $Ag_2Ge_{48}Te_{50}$. Similarly, if Sb results in less Ge vacancies, $\sim 1 \times 10^{20}$ cm^{-3} ($\sim 0.5\%$) Ge vacancies are needed to explain a decrease in the carrier concentration in $Sb_2Ge_{48}Te_{50}$. All scenarios shown above seem to be realistic.

Selbach *et al.* [18] also showed dependencies containing the carrier effective mass m^*, $1/T_1 \sim (m^*)^{3/2}n$ with Maxwell-Boltzmann statistics or $1/T_1 \sim (m^*)^2n^{2/3}$ with Fermi-Dirac statistics, which demonstrate that m^* can also affect the relation between T_1 and n, and needs to be studied in more detail. However, the large shifts in the ^{125}Te NMR spectra correlate well with the changes in T_1, showing that a major effect on T_1 in $Ag_xGe_{50-x}Te_{50}$ and $Sb_xGe_{50-x}Te_{50}$ arises from the carrier concentration. Note also that the T_1 values across the ^{125}Te NMR spectrum in GeTe change insignificantly, showing that the large broadening 460 ppm cannot be attributed only to the distribution of Knight shifts.

The position of the NMR signal in electrically conductive materials is typically expressed via the total shift δ_{total} relative to the reference material: $\delta_{total} = \delta_{chem} + K$, where δ_{chem} is the chemical shift due to the environment around the Te atoms and K is the Knight shift due to the effect of the hyperfine interaction between nuclei and free (mobile) charge carriers and strongly depends on the carrier concentration [18,19]. The Knight shift K and spin-lattice relaxation time T_1 are related via the Korringa relation $K^2T_1T = $ const, where T is the absolute temperature [19] and at constant temperature the Korringa relation can be shown as $K^2T_1 = $ constant [21].

Note that GeTe, $Ag_xGe_{50-x}Te_{50}$, and $Sb_xGe_{50-x}Te_{50}$ show diamagnetic properties in a temperature range of 1.8–300 K and magnetic fields of 0–50 kOe (data not shown), which allows us to conclude that the Korringa mechanism of relaxation is the dominant one. Measurements of T_1 enable us to estimate the contributions to the resonance positions from K and δ_{chem} in $Ag_xGe_{50-x}Te_{50}$ and $Sb_xGe_{50-x}Te_{50}$. At the same temperature $K = K_r(T_{1,r}/T_1)^{1/2}$ where K_r and $T_{1,r}$ are the Knight shift and spin-lattice relaxation time of a reference material GeTe. The Knight shift of GeTe can be determined as $K = \delta_{total} - \delta_{chem}$, where $\delta_{total} = +160\,ppm$ [8] and $\delta_{chem} = -890\,ppm$ [22] so $K = +1050\,ppm$. The Knight shift estimated from T_1 for $Ag_2Ge_{48}Te_{50}$ is about $+1700\,ppm$ and for $Sb_2Ge_{48}Te_{50}$ using long T_1 components is $+600\,ppm$, i.e., they are larger and smaller, respectively, than that of GeTe, which explains the position of ^{125}Te NMR signals (Fig. 3).

In general, Ag in GeTe serves as a donor, whereas Sb serves as an acceptor. However, the effect of chemical substitution via alloying in GeTe is quite different compared to that in semiconductors, such as Si, where donors (P) create mobile electrons (n-type conductivity) directly in the conduction band, whereas acceptors (B) create mobile holes (p-type conductivity) in the valence band. Although GeTe is a semiconductor, the temperature dependence of its electrical resistivity is typical for that of metals up to 800 K [8], which can be explained by a high-carrier concentration generated by Ge vacancies [7]. $Ag_xGe_{50-x}Te_{50}$ and $Sb_xGe_{50-x}Te_{50}$ also exhibit metallic conductivity (not shown here), which demonstrates that the analysis of these materials can be conducted upon the assumption of a degenerate electronic (metallic) state in these materials [23].

Opposite changes in carrier concentration in $Ag_xGe_{50-x}Te_{50}$ and $Sb_xGe_{50-x}Te_{50}$ can be explained by different valence electron configurations of Ag and Sb compared to that of Ge, which results in a different local electron imbalance and/or in a change in Ge vacancy formation energy, and affects the total carrier concentration. Density functional theory calculations for pure GeTe by Edwards *et al.* [24] show that: (i) Ge vacancy has very low formation energy, and (ii) the presence of Ge vacancies in large numbers leads to a large concentration of holes in the valence band. In principle, Ag can also decrease this energy, whereas Sb can increase it, and this may result in a higher or lower concentration of Ge vacancies and change the total carrier concentration.

A total hole concentration p_{total} in GeTe-based materials containing Ag or Sb may consist of contributions from (i) Ge vacancies (two holes per vacancy) producing the base hole concentration p_{base} and dependent mostly on the Ge/Te ratio, (ii) due to Ag at a Ge site producing an additional hole and/or more Ge vacancies and resulting in $p_{total} > p_{base}$, and (iii) due to Sb at a Ge site producing one electron and due to its compensation in a p-type GeTe matrix and/or less Ge vacancies resulting in $p_{total} < p_{base}$. In $Ag_2Sb_2Ge_{46}Te_{50}$ the numbers of Ag and Sb atoms are nearly equal, and $p_{total} \approx p_{base}$, which follows from both the value of the Seebeck coefficient and

the ^{125}Te NMR data. Nevertheless, the replacement of Ge in GeTe by Ag or Sb can significantly increase or decrease, respectively, the free carrier concentration [Fig. 4(a)].

Our data for the Seebeck coefficient of electronically homogeneous $Ag_xGe_{50-x}Te_{50}$ system can be explained, in general, using the $S \sim 1/n^{2/3}$ dependence. Note that the values of the Seebeck coefficient calculated using the carrier concentration extracted from T_1 NMR analysis with the Maxwell-Boltzmann statistic fit better than those obtained with Fermi-Dirac statistics. Data for the electronically inhomogeneous $Sb_xGe_{50-x}Te_{50}$ system show that the observed larger Seebeck coefficient (Fig. 1) should be attributed mostly to the charge carriers of the lower concentration (associated with longer T_1); some effect from the carriers of the higher concentration (associated with shorter T_1) cannot be excluded.

The carrier concentration in both $Ag_xGe_{50-x}Te_{50}$ and $Sb_xGe_{50-x}Te_{50}$ changes nonlinearly showing a limitation in the solubility of Ag and Sb. The carrier concentration in $Ag_2Sb_2Ge_{46}Te_{50}$ calculated using $T_1 = 3.6\,ms$ [12] is $12 \times 10^{20}\,cm^{-3}$, just slightly larger when compared to that in GeTe [Fig. 4(a)]. Similarly, the values of the Seebeck coefficient and electrical resistivity [Figs. 2(a) and 2(b)] are close to those in GeTe. Interplay between the Seebeck coefficient and the electrical resistivity in $Ag_xGe_{50-x}Te_{50}$ and $Sb_xGe_{50-x}Te_{50}$ alloys significantly affects the power factor [Fig. 4(b)]. The largest value of $PF = 46\,\mu W\,cm^{-1}\,K^{-2}$ was found for $Sb_2Ge_{48}Te_{50}$, which is even higher than that of GeTe $42\,\mu W\,cm^{-1}\,K^{-2}$ reported in Ref. [8] and confirmed by Sun *et al.* [25], and is one of the highest values observed for high-efficiency thermoelectric tellurides.

To summarize, the replacement of Ge in a p-type self-doping GeTe semiconductor by Ag or Sb in $Ag_xGe_{50-x}Te_{50}$ or $Sb_xGe_{50-x}Te_{50}$ alloys forms solid solutions with an insignificant amount of separate phases. Ag decreases the Seebeck coefficient whereas Sb increases it, which according to ^{125}Te NMR spectra and spin-lattice relaxation time can be explained by the respective increase or decrease in the carrier concentration. Two approaches based on Maxwell-Boltzmann (for semiconductors) and Fermi-Dirac (for metals) statistics, which describe the relation between the carrier concentration and the NMR spin-lattice relaxation time, were used to calculate the carrier concentration and showed similar trends. Comparison of our data for GeTe, $Ag_2Ge_{48}Te_{50}$, and $Sb_2Ge_{48}Te_{50}$ with those for $Ag_2Sb_2Ge_{46}Te_{50}$ shows that the effects from Ag and Sb compensate for each other and supports the formation of $[Ag + Sb]$ atomic pairs suggested earlier based on theoretical calculations.

[1] G. J. Snyder and E. S. Toberer, Nature Mater. **7**, 105 (2008).

[2] E. A. Skrabek and D. S. Trimmer, in *CRC Handbook of Thermoelectrics*, edited by D. M. Rowe (CRC, Boca Raton, FL, 1995), Chap. 22.

[3] S. H. Yang, T. J. Zhu, T. Sun, J. He, S. N. Zhang, and X. B. Zhao, Nanotechnology **19**, 245707 (2008).

[4] J. R. Salvador, J. Yang, X. Shi, H. Wang, and A. A. Wereszczak, J. Solid State Chem. **182**, 2088 (2009).

[5] E. M. Levin, S. L. Bud'ko, and K. Schmidt-Rohr, Adv. Funct. Mater. **22**, 2766 (2012).

[6] P. M. Nikolic, Br. J. Appl. Phys. **2**, 383 (1969).

[7] M. S. Lubell and R. Mazelsky, J. Electrochem. Soc. **110**, 520 (1963).

[8] E. M. Levin, M. F. Besser, and R. Hanus, J. Appl. Phys. **114**, 083713 (2013).

[9] T. Chattopadhyay, J. X. Boucherle, and H. G. von Schnering, J. Phys. C: Solid State Phys. **20**, 1431 (1987).

[10] E. M. Levin, J. P. Heremans, M. G. Kanatzidis, and K. Schmidt-Roh, Phys. Rev. B **88**, 115211 (2013).

[11] R. Wolfe, J. H. Wernick, and E. Haszko, J. Appl. Phys. **31**, 1959 (1960).

[12] E. M. Levin, R. Hanus, M. Hanson, W. E. Straszheim, and K. Schmidt-Rohr, Phys. Status Solidi A **210**, 2628 (2013).

[13] K. Hoang, S. D. Mahanti, and M. G. Kanatzidis, Phys. Rev. B **81**, 115106 (2010).

[14] H. Hazama, U. Mizutani, and R. Asahi, Phys. Rev. B **73**, 115108 (2006).

[15] N. Chen, F. Gascoin, G. J. Snyder, E. Müller, G. Karpinski, and C. Stiewe, Appl. Phys. Lett. **87**, 171903 (2005).

[16] A. Kosuga, K. Kurosaki, H. Muta, C. Stiewe, G. Karpinski, E. Muller, and S. Yamanaka, Mater. Trans. **47**, 1440 (2006).

[17] E. M. Levin, B. A. Cook, K. Ahn, M. G. Kanatzidis, and K. Schmidt-Rohr, Phys. Rev. B **80**, 115211 (2009).

[18] H. Selbach, O. Kanert, and D. Wolf, Phys. Rev. B **19**, 4435 (1979).

[19] J. P. Yesinowski, Top Curr. Chem. **306**, 229 (2012).

[20] Y. Gelbstein, B. Daro, O. Ben-Yehuda, Y. Sadia, Z. Dashevsky, and M. P. Dariel, J. Electron. Mater. **39**, 2049 (2010).

[21] J. P. Yesinowski, A. P. Purdy, H. Wu, M. G. Spencer, J. Hunting, and F. J. DiSalvo, J. Am. Chem. Soc. **128**, 4952 (2006).

[22] B. Njegic, E. M. Levin, and K. Schmidt-Rohr, Solid State Nucl. Magn. Reson. **55-56**, 79 (2013).

[23] R. Shaltaf, X. Gonze, M. Cardona, R. K. Kremer, and G. Siegle, Phys. Rev. B **79**, 075204 (2009).

[24] A. H. Edwards, A. C. Pineda, P. A. Schultz, M. G. Martin, A. P. Thompson, H. P. Hjamarson, and C. J. Umrigar, Phys. Rev. B **73**, 045210 (2006).

[25] H. Sun, X. Lu, H. Chi, D. T. Morelli, and C. Uher, Phys. Chem. Chem. Phys. **16**, 15570 (2014).